Electron spin transport in graphene and carbon nanotubes

Tombros, Nikolaos

4

Separating spin and charge transport in single wall carbon nanotubes[1]

We demonstrate spin injection and detection in single wall carbon nanotubes using a 4-terminal, non-local geometry. This measurement geometry completely separates the charge and spin circuits. Hence all spurious magnetoresistance effects are eliminated and the measured signal is due to spin accumulation only. Combining our results with a theoretical model, we deduce a spin polarization at the contacts, α_F, of approximately 25 %. We show that the magnetoresistance changes measured in the conventional two-terminal geometry are dominated by effects not related to spin accumulation.

[1]Published as: N.Tombros, S.J. van der Molen, and B. J. van Wees, Phys. Rev. B, **73**, 233403 (2006)

4.1 Introduction

Single wall carbon nanotubes (SWNTs) behave as almost ideal one-dimensional conductors, having a small diameter (typically a nanometer) on the one hand, and a large scattering mean free path on the other hand [1]. Additionally, it is expected that electronic spin flip scattering in SWNTs is weak. This makes them excellent candidates for spintronic devices, in which the nanotubes are contacted by ferromagnetic leads. Despite the promise that the combination of nanotubes and spintronics holds, there have been no experiments so far that unequivocally demonstrate spin accumulation in carbon nanotubes. In fact, all experiments performed since the pioneering work of Tsukagoshi *et al.* [2], have made use of the conventional two-terminal spin valve geometry [3–9]. Unfortunately, in this geometry, it is difficult to separate spin transport from other effects, such as Hall effects, anisotropic magnetoresistance [10, 11], interference effects [12] and magneto-coulomb effects [13]. These may obscure and even mimic the spin accumulation signal. With a four-terminal non-local spin valve geometry [10, 14, 15], one is able to completely separate the spin current path from the charge current path. Hence, the signal measured is due to spin transport only. With this technique we unambiguously demonstrate spin accumulation in single wall carbon nanotubes.

4.2 Non-local spin transport in a single wall nanotube

To determine spin accumulation in the non-local geometry (see Fig. 4.1c, one needs to contact a metallic SWNT with four electrodes. At least two of these should be ferromagnetic. They act as spin injector and spin detector, respectively. For practical reasons, we make use of four ferromagnetic contacts. These electrodes are narrow, but of different widths to assure different switching fields B_C(B_C decreases with increasing width) [10, 15]. Single wall carbon nanotubes (>90% SWNT, from Nanostructured Amorphous Materials, Inc) are dispersed in HPLC grade chlorobenzene. We use the alternating current dielectrophoresis technique [16] to deposit the SWNT's at a predefined area on the substrate. An atomic force microscope (AFM) in tapping mode is used to locate and characterize the SWNT's on the SiO_2 surface. Conventional electron beam lithography and e-beam evaporation (45 nm of Co at $4.0 \cdot 10^{-7}$ mbar) are used to define the contacts. To avoid damaging the nanotube, no additional cleaning is done before deposition.

Although we regularly obtain low contact resistances ($\sim$kΩ), the preparation of

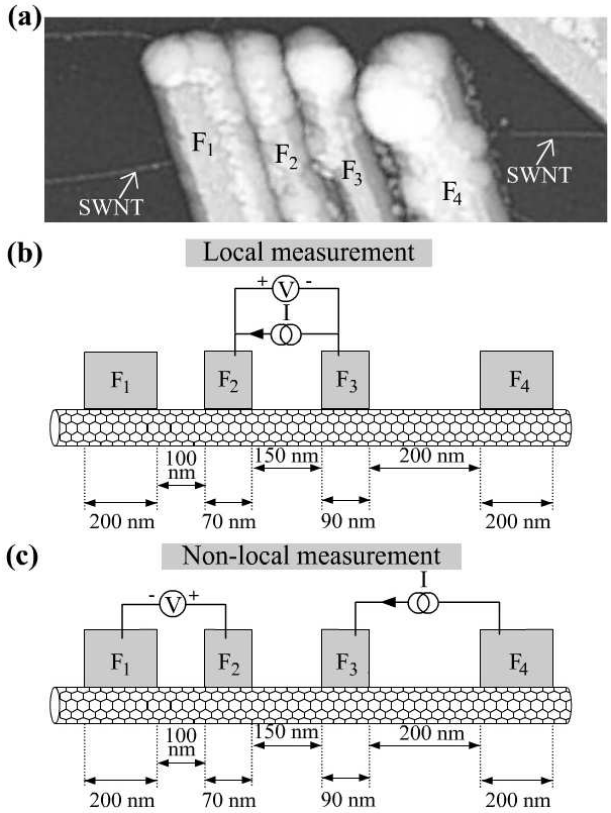

Figure 4.1: A single wall carbon nanotube (d=3.4 ±0.4 nm; possibly it is a bundle containing a few nanotubes) contacted by four ferromagnetic (cobalt) electrodes. (a) An AFM picture of the device. Note that imperfect lift-off resulted in some PMMA residue on top of the cobalt electrodes, this partially obscures the well defined Co electrodes underneath. We independently checked that this does not provide an extra current path (see also A.Javey *et al.* [20] (b) Geometry of a conventional spin valve (or 'local') measurement, in which contacts F_2 and F_3 are used both to inject current and to measure voltage. (c) The 'non-local' geometry. In this case the voltage circuit (F_1-SWNT-F_2) is completely separated from the current circuit (F_3-SWNT-F_4)

the device is not trivial, as all the contacts have to be low ohmic. It is also crucial that electron and spin transport can occur through the entire nanotube, including the regions underneath the Co contacts. Out of 15 devices, we obtained one device that fulfilled these requirements. In Fig. 4.1 it is depicted. The two outermost electrodes, F_1 and F_4, have a width of 200 nm. The two central electrodes, F_2

and F_3, have a width of 70 nm and 90 nm, respectively. The nanotube itself has a diameter of 3.4 ± 0.4 nm (we cannot exclude that it is a bundle containing a few SWNT's). To measure the transport properties of the nanotube, we make use of a standard a.c. lock-in technique (maximum current: 60 nA). At 4.2 K, we find two-terminal resistances of 28 kΩ, 12.4 kΩ, 15 kΩ, 44.3 kΩ, 22.8 kΩ and 52.6 kΩ between contacts F_1-F_2, F_2-F_3, F_3-F_4, F_1-F_3, F_2-F_4 and F_1-F_4, respectively. A four-terminal measurement (current from F_1 to F_4; voltage between F_2 and F_3) gives a resistance of 10.3 kΩ, equivalent to a conductance of $2.5 \cdot e^2/h$. Since these values are quite close to $4e^2/h$, we are probing at least one metallic (or degenerate semiconductor) SWNT. From the values above, we deduce the contact resistances between the nanotube and electrodes F_2 and F_3. Comparing the four-terminal resistance with the two-terminal measurement (F_2-F_3), we get values around a kΩ.

Next, we investigate the two-terminal 'spin valve' effect between contacts F_2 and F_3 (see Fig. 4.1b). For this, we continuously sweep the magnetic field back and forth between -165 mT and 165 mT (at 4.2 K). Two characteristic traces are shown in Fig. 4.2a. The behavior found is generally described as follows. Let us start at $B = 165mT$, where F_2 and F_3 are both magnetized parallel to the external field. When the field is subsequently swept to negative values, F_3 (being the widest) will flip magnetization as soon as the external field equals its switching field. Consequently, the magnetizations of F_2 and F_3 are now anti-parallel, leading to a resistance increase. When the B-field gets more negative, also F_2 switches, so that the magnetizations of both are parallel again. This leads to a resistance decrease, back to the original value. A magnetoresistance change of approximately 6 % is observed in Fig. 4.2a. This is a considerable effect, comparable to the values reported in Ref. [2] ($\leq 9\%$).

Although it appears that Fig.4.2a can be explained as a result of spin transport only, we argue that this is not the case. Figure 4.2b shows an experiment performed on the same sample in the exact same measurement geometry, at 4.2 K. (There is a thermal cycling step in between Fig. 4.2a and b.) A completely different behavior is observed. A predominantly negative, instead of positive, magnetoresistance signal is now seen at positive B-fields. Similar negative magnetoresistances have been observed in multiwall carbon nanotubes [5–7]. It is non-trivial to explain these effects from spin transport only (they would require a sign change in the polarization at only one of the electrodes) [17]. Another curiosity, often observed in nanotubes (although not by us), is the fact that the magnetoresistance increases before the external field has even changed sign [2, 5, 11]. The problem in the interpretation lies in the fact that many other phenomena, not related to spin, influence the magnetoresistance [10–13]. Without extra knowledge these are inseparable from spin accumulation in a two-terminal experiment.

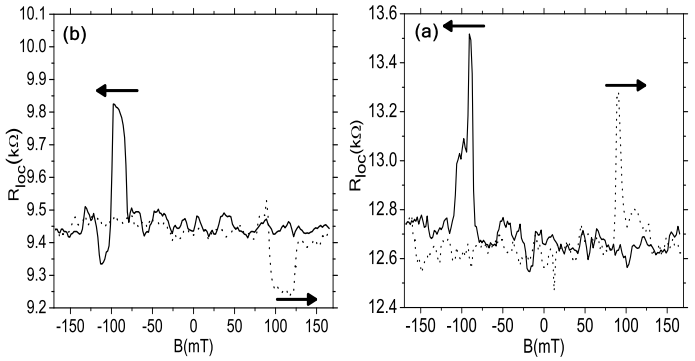

Figure 4.2: Two-terminal spin valve measurements (F_2-SWNT-F_3, I = 10nA) at 4.2 K (see Fig. 4.1b. (a) Upon sweeping the B-field, the 'local' resistance increases when B reaches $\approx 80mT$. It falls back to its original value when B increases further. ΔR/R has a maximum value of $\approx 6\%$. We observe significant substructure on top of the resistance peaks. (b) A similar measurement on the same sample (also at 4.2 K, but with a thermal cycling step in between). The magnetoresistance trace is completely different from the traces in a) and shows both positive and negative values for ΔR/R.

Fortunately, spin accumulation can be isolated from spurious effects by adopting the non-local measurement geometry (see Fig. 4.1c) [10, 14, 15]. In such experiments, the *charge* current path is completely separated from the *spin* current path. In our case, this is done by attaching the current probes to F_3 (I^+) and F_4 (I^-) and the voltage probes to F_2 (V^+) and F_1 (V^-), thus measuring the 'non-local' magneto-resistance $R_{non-loc} \equiv (V^+ - V^-)/I$. In Fig. 4.3a and c, we display two sets of measurements. A clear and clean switching behavior is seen for all traces. These results are similar to those obtained by Jedema *et al.* for Al wires [15]. Characteristic is the change of sign from positive (+15 Ω) to negative (-5 Ω) resistance values. This sign change can only happen if the voltage probe F_2 ('detector') measures spin accumulation in the SWNT system. In fact, when the voltage probe F_2 is parallel to the spin 'injector' F_3, it probes the (positive) electrochemical potential of the majority spin species (giving positive non-local resistance). However, when its magnetization is anti-parallel to that of F_3, it

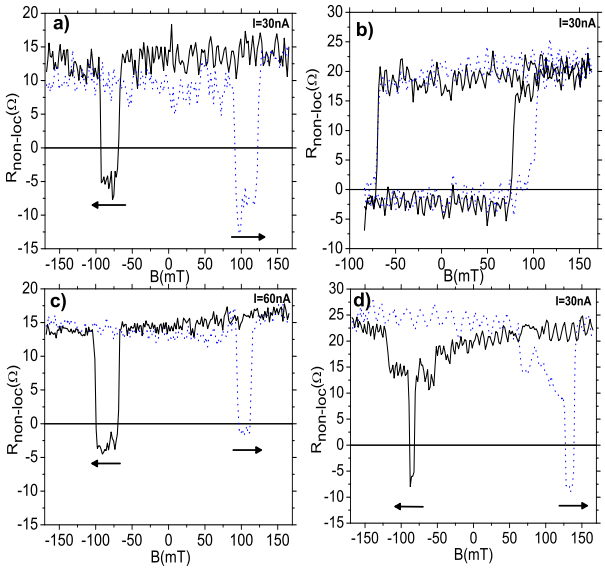

Figure 4.3: Non-local measurements at T=4.2 K. The current path (from F_3 to F_4) is separated from the voltage probes (F_2 to F_1, see Fig. 4.1c. The observed resistance switching is due to spin accumulation and spin transport in the single wall carbon nanotube. a) Full magnetic field scan with an a.c. current of 30 nA. $R_{non-loc}$ is negative when the spin injector, F_3, is magnetized antiparallel to the spin detector, F_2. In this situation the detector measures mainly the negative chemical potential of the minority spin species. (b) The memory effect (I=30 nA), in which only the magnetization of F_3 is switched.(c) Similar measurement to a), but now with an a.c. current of 60 nA, resulting in a reduction of the resistance noise level. (d) Non-local measurement similar to (a), with I=30 nA. Between (a)-(c), and (d), respectively, the sample was annealed to room temperature.

probes the (negative) chemical potential of the minority spins. The change of sign thus assures us that we are measuring spin accumulation (ruling out more complicated current paths such as observed in multiwall nanotubes) [18]. We note that an important feature in Fig. 4.3 is the reduction of the noise ($\approx$3 Ω), as compared to Fig. 4.2 ($\approx$50 Ω). This illustrates the insensitivity of non-local measurements with respect to fluctuations in the overall resistance.

As an extra confirmation, we measure the so-called 'memory effect' in the non-local geometry (Fig. 4.3b). This hysteresis effect is generated by allowing

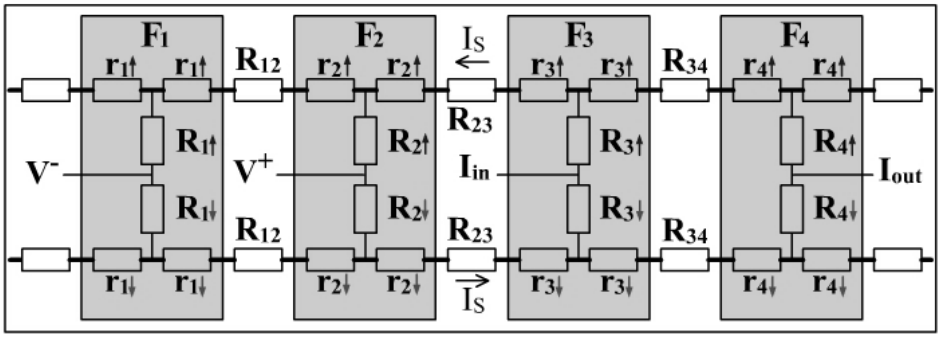

Figure 4.4: A resistor model of our system (here, all four electrodes are assumed magnetized in the 'up' direction). The upper half of the resistor network corresponds to the spin up (↑) transport channel in the nanotube. The lower half to the spin down (↓) channel. The resistance of the carbon nanotube between the cobalt contacts F_1-F_2, F_2-F_3 and F_3-F_4 is equal to $R_{12}/2$, $R_{23}/2$ and $R_{34}/2$, respectively. The contact between the carbon nanotube and ferromagnet F_i (i=1,2,3,4) can be represented by a number of spin-dependent resistances $R_{i,\eta}$ and $r_{i,\eta}$, where $\eta = \uparrow, \downarrow$ denotes spin. Assuming spin up to be the majority species, we have $R_{i,\uparrow} < R_{i,\downarrow}$ and $r_{i,\uparrow} < r_{i,\downarrow}$. Due to the spin-dependent resistances in the current circuit (F_3 and F_4), the charge current I produces a finite spin current I_S. Due to the spin-dependent resistances in the voltage circuit (F_1 and F_2), a non-zero voltage difference $V^+ - V^-$ consequently develops, leading to a finite non-local resistance $R_{non-loc} \equiv (V^+ - V^-)/I$.

only one of the two central electrodes to switch. We start at B=165 mT for which the magnetizations of F_2 and F_3 are parallel and the non-local resistance is positive. Subsequently, we decrease the magnitude of the applied magnetic field to negative values until F_3 switches at ≈ -70mT. Now F_2 and F_3 are anti-parallel and $R_{non-loc}$ becomes negative. Next, we sweep to positive fields again (F_2, F_3 are still anti-parallel) until at ≈70 mT electrode F_3 switches back. Thus we have returned to the original situation. This demonstrates that the magnetization of one individual electrode determines the sign of the measurement. Finally in Fig. 4.3d we show a non-local resistance measurement (at 4.2 K, cf. 4.3a after annealing to room temperature. Again we observe a change of sign in $R_{non-loc}$.

4.3 Discussion and conclusions

Comparing Fig. 4.2a with Fig. 4.3a, an interesting observation can be made. Whereas in the conventional spin valve measurement a magnetoresistance change

$\Delta R_{loc} \approx 700\Omega$ is found, the 'non-local' experiment yields $\Delta R_{non-loc} = 20\Omega$, i.e., only 3 % of the 'local' value. This raises the question if the large spin valve effect in Fig. 4.2 originates from spin accumulation or from spurious phenomena. To answer this, we model the spin imbalance within the nanotube using a resistor network (see Fig. A.1). This model is discussed in Appendix *A*. We assume the spin flip length, λ_{sf} to exceed all sample dimensions. The (spin-independent) nanotube resistance between contacts i and $i+1$ is denoted by $R_{i,i+1}$. The contact resistance at each electrode is split in two spin-dependent terms: $r_{i,\eta}$ and $R_{i,\eta}$ (where $\eta = \uparrow, \downarrow$ denotes spin direction). Both are calculated, assuming a contact conductivity $\sigma_{\uparrow(\downarrow)} = \sigma_0(1 \pm \alpha_F)/2$, where $0 < \alpha_F < 1$ denotes the spin polarization. We have measured all possible combinations of two-, three- and four-probe resistances in the SWNT device. From this we can determine the contact resistances between the nanotube and contacts F_2 and F_3. The contact resistances between the nanotube and contacts F_1 and F_4 cannot be precisely determined and are assumed equal to those of F_2 and F_3. From the model, the contact resistances, and the non-local traces, we obtain a spin polarization $\alpha_F \approx 0.25$. Given the assumptions of our model we estimate that the obtained parameters are accurate within a factor of two. We note that this is only a factor of two smaller than what is ideally attainable. This indicates that the assumption of λ_{sf} being large in a carbon nanotube is justified. Now, one can also calculate the expected 'local' resistance change, giving $\Delta R_{loc} \approx 70\Omega$ [19]. Consequently, around 90 % of the resistance change in Fig. 4.2 cannot be attributed to spin accumulation. This demonstrates how easily spin accumulation is masked by other effects [10, 15]. Interestingly, from the resistor model, another phenomenon can be understood: the influence of F_1 and F_4 on the non-local measurement is rather small. The reason is that the contribution due to these contacts is attenuated by a factor of roughly $R_{i,\eta}/R_{i,i+1}$. For the measurements in Figs. 4.3a-c, we estimate the effect of the outer electrodes' switching to be $\approx 1\Omega$ (deduced from our set of resistance values). This lies within the measurement noise. After annealing to room temperature, however (see Fig. 4.3d), the resistances have changed somewhat. Not only does this lead to a higher non-local resistance change (30 Ω), we also observe a small extra step. We relate this extra jump to magnetization switching of contacts F_1 and F_4.

Summarizing, we use a non-local measurement geometry to separate spin transport from charge transport in a single wall carbon nanotube contacted by ferromagnets. In this way, we unambiguously demonstrate spin accumulation in a carbon nanotube device. Not only does this work lead to a better understanding for future spin-based nanotube applications, it also opens the road to more sophisticated spin experiments on nanotubes (e.g. precession measurements and/or determination of the spin flip length, λ_{sf}, in carbon nanotubes).

References

[1] R. H. Baughman, A. A. Zakhidov, W. A. de Heer, *Science* **297**, 787 (2002).

[2] K. Tsukagoshi, B. W. Alphenaar and H. Ago, *Nature* **401** 572 (1999).

[3] K. Tsukagoshi and B. W. Alphenaar, *Superlattices and Microstructures* **27**, 565 (2000).

[4] J. R. Kim, *et al.*, *Phys. Rev. B.* **66**, 233401 (2002).

[5] S. Chakraborty, *et al.*, *App. Phys. Lett* **83**, 1008 (2003).

[6] D. Orgassa, G. J. Mankey and H. Fujiwara, *Nanotechnology* **12**, 281 (2001).

[7] B. Zhao, *et al.*, *Jour. Appl. Phys.* **91**, 7026 (2002)

[8] S. Sahoo, *et al.*, *Appl. Phys. Lett.* **86**, 112109 (2005)

[9] A. Jensen, thesis, Technical University of Denmark and University of Copenhagen, Copenhagen, Denmark (2003)

[10] F. J. Jedema, A. T. Filip and B. J. van Wees, *Nature* **410**, 345 (2001).

[11] B. W. Alphenaar, S. Chakraborty and K. Tsukagoshi, in *Electron Transport in Quantum Dots* (Kluwer Academic/Plenum Publishers, New York 2003) chap. 11.

[12] H. T. Man and A.F. Morpurgo, *Phys. Rev. Lett.* **95**, 026801 (2005)

[13] K. Ono, H. Shimada and Y. Ootuka, *J. Phys. Soc. Jpn* **67**, 2852 (1998); H. Shimada, K. Ono, and Y. Ootuka, *J. Appl. Phys.* **93**(10), 8259 (2003)

[14] M. Johnson and R.H. Silsbee, *Phys. Rev. Lett.* **55**, 1790 (1985)

[15] F. J. Jedema, *et al.*, *Nature* **416**, 713 (2002)

[16] R. Krupke, *et al.*, *Science* **301**, 344 (2003)

[17] S. Krompiewski, *Phys. stat. sol. (b)* **2**, 226 (2005)

[18] B. Bourlon, *et al.*, *Phys. Rev. Lett.* **93**, 176806 (2004).

[19] F. J. Jedema, *et al.*, *Phys. Rev. B* **67**, 085319 (2003)

[20] A. Javey, *et al.*, *Nature* **424**, 654 (2003)